DOE/BC/14896--19

GEOLOGICAL AND PETROPHYSICAL CHARACTERIZATION OF THE FERRON SANDSTONE FOR 3-D SIMULATION OF A FLUVIAL-DELTAIC RESERVOIR

(Contract No. DE-AC22-93BC14896) R/3

BC/14896-19

Utah Geological Survey (UGS), Salt Lake City, Utah 84114

Submitted: March 1997

4Q/96

Contract Date: September 29, 1993

Anticipated Completion Date: August 28, 1997

Government Award (fiscal year): $ 61,648

Principal Investigator: M. Lee Allison, UGS

Program Manager: Thomas C. Chidsey, Jr., UGS

Contracting Officer's Representative: Robert Lemmon, National Petroleum Technology Office, Bartlesville, Oklahoma

Reporting Period: October 1 - December 31, 1996

RECEIVED
APR 15 1998
OSTI

Objective

The objective of this project is to develop a comprehensive, interdisciplinary, and quantitative characterization of a fluvial-deltaic reservoir which will allow realistic inter-well and reservoir-scale modeling to be constructed for improved oil-field development in similar reservoirs world-wide. The geological and petrophysical properties of the Cretaceous Ferron Sandstone in east-central Utah will be quantitatively determined. Both new and existing data will be integrated into a three-dimensional representation of spatial variations in porosity, storativity, and tensorial rock permeability at a scale appropriate for inter-well to regional-scale reservoir simulation. Results could improve reservoir management through proper infill and extension drilling strategies, reduction of economic risks, increased recovery from existing oil fields, and more reliable reserve calculations. Transfer of the project results to the petroleum industry is an integral component of the project.

DISTRIBUTION OF THIS DOCUMENT IS UNLIMITED

MASTER

DISCLAIMER

This report was prepared as an account of work sponsored by an agency of the United States Government. Neither the United States Government nor any agency thereof, nor any of their employees, makes any warranty, express or implied, or assumes any legal liability or responsibility for the accuracy, completeness, or usefulness of any information, apparatus, product, or process disclosed, or represents that its use would not infringe privately owned rights. Reference herein to any specific commercial product, process, or service by trade name, trademark, manufacturer, or otherwise does not necessarily constitute or imply its endorsement, recommendation, or favoring by the United States Government or any agency thereof. The views and opinions of authors expressed herein do not necessarily state or reflect those of the United States Government or any agency thereof.

DISCLAIMER

Portions of this document may be illegible electronic image products. Images are produced from the best available original document.

Summary of Technical Progress

Four activities continued this quarter as part of the geological and petrophysical characterization of the fluvial-deltaic Ferron Sandstone in the Ivie Creek case-study area (Fig. 1): (1) geostatistics, (2) field description of clinoform bounding surfaces, (3) reservoir modeling, and (4) technology transfer.

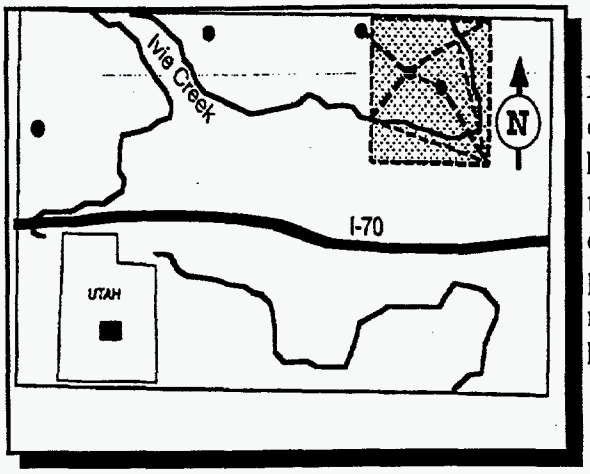

Fig. 1. Sketch map of Ivie Creek case-study area showing the location of modeling domains used to simulate fluid flow through clinoform lithofacies of the Kf-1-Iv parasequence set. Black dots represent project drill-hole locations.

Geostatistics

Geostatistical work this quarter included: (1) displaying in illustrations the deterministic permeability of the Ferron Sandstone No. 1 Ivie Creek-a parasequence (Kf-1-Iv-a) and (2) testing the permeability data set for log normality.

Deterministic permeability panels consisted of two models (Fig. 2). The first model incorporated clinoform proximal, medial, and distal lithofacies as the sole control on permeability distribution (Fig. 2A). The second model incorporated lithofacies, sedimentary structure, and average grain size to distribute permeability values (Fig. 2B). Each block in the model was populated with the geometric mean of the permeability data as a function defining parameters of that block.

The Lilliefors test was used to analyze the permeability data set for log normality since it could handle the large number of data points involved and is considered to be one of the more robust tests available. Of the 41 categories that permeability data were divided into, only nine categories met the criteria of log normality. Categories fail due to two factors: (1) the large number of data points which cause the cumulative probability curve to be highly constrained so even a small deviation away from log normality will result in test failure, and (2) the limits of the permeability instruments (0.5 and 2.0 millidarcies [md]) which create step increases in the cumulative probability curves. The influence of the second factor is evident when the Kf-1-Iv-a permeability data were modeled to remove instrument effects. The modeled data sets (Fig. 3) pass the log-normality test.

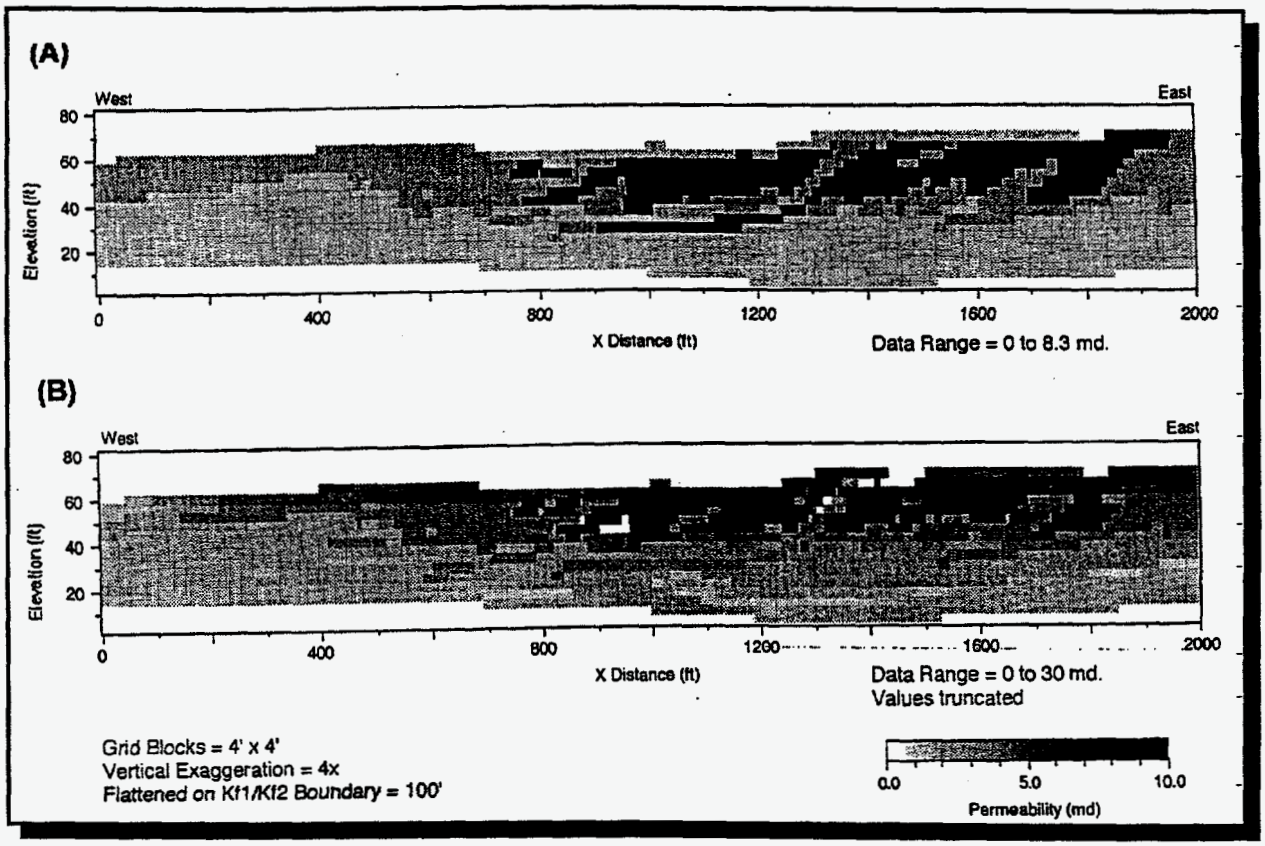

Fig. 2. Ivie Creek amphitheater two-dimensional deterministic model for the Kf-1-Iva parasequence. (A) Geometric mean permeability distribution incorporating only lithofacies. (B) Geometric mean permeability distribution incorporating lithofacies sedimentary structure, and average grain size.

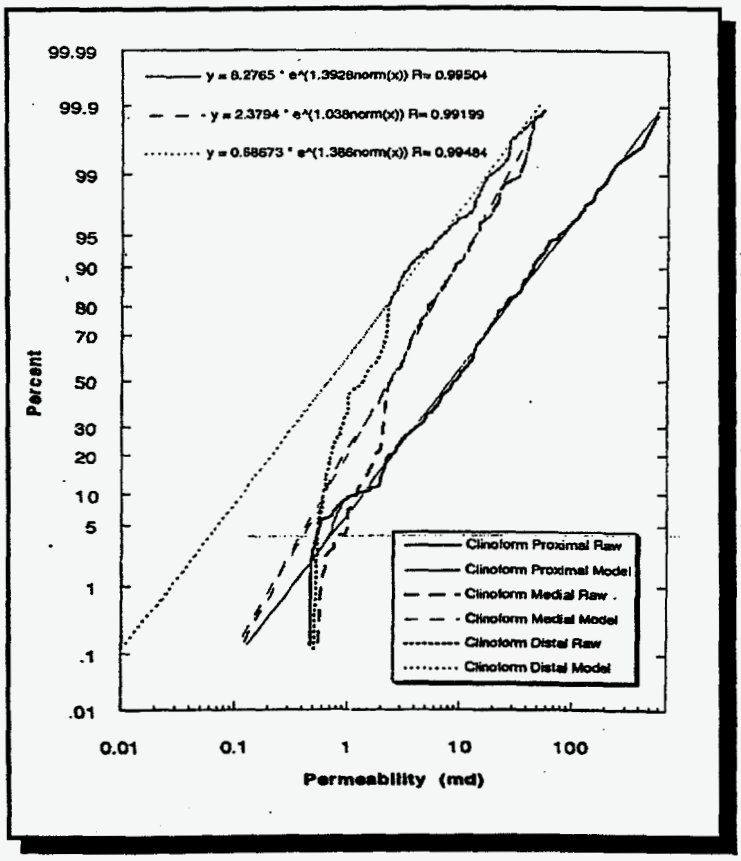

Fig. 3. Cumulative probability curves of lithofacies vs. permeability model and raw data for the Kf-1-Iv-a parasequence of the detailed scale model.

Variograms were created for the parasequence surfaces mapped in the Kf-1-Iv and Kf-2-Iv parasequence sets (Fig. 4). The variograms provided spatial relationships as an input to ordinary kriging. Each of the surfaces was kriged and then smoothed (500 ft operator) in an attempt to remove artifacts. These steps will result in a set of elevation and isopach maps.

Field Description of Clinoform Bounding Surfaces

Descriptive field data were gathered to better define the flow characteristic across clinoform-to-clinoform boundaries in the Kf-1-Iv-a parasequence in the Ivie Creek case-study area. The emphasis was on bounding surfaces in portions of the clinoforms which are designated proximal or medial lithofacies. It was assumed that the distal lithofacies in the clinoforms are all similar in permeability and essentially act as strong baffles or barriers to flow.

The measured section data, photomosaics, and overlaying line work (which defines the clinoforms and lithofacies), and permeability transect data were used to target specific clinoforms for study. Bounding surfaces were described with the following information: location (plotted on the photomosaic), type of bounding surface (between what lithofacies), thickness of the feature, slope profile, detailed description of the rocks which comprise the thickness of the bounding surface, a general description of the rocks above and below the bounding surface, photographs of the surface and the overlying and underlying rock, and geologists' in-field opinion of the cause of the bounding surface.

Twenty-two bounding-surface locations were examined and described. From these field examinations, it was determined that what has been referred to as a surface has a third dimension and varies from a true two-dimensional plane at the tops of the clinoforms to a planar body with increasing thickness in a down-depositional dip direction. Most of the examined bounding surfaces contained two common lithologic elements: (1) finer-grained, poorer cemented, and less resistant lithology than the overlying and underlying units, and (2) laminations of carbonaceous material which are consistently poorly cemented and become planes of weakness which are expressed in the recessive outcrops of the bounding surfaces. Most of the bedding in the bounding surfaces was horizontal to slightly irregular. On occasion clearly recognizable wave-ripple laminations were found along with some flaser bedding. Often some portion of the bounding surface contained gypsum veinlets.

Bounding surfaces found associated with a proximal-to-proximal lithofacies contact were generally somewhat thinner than those associated with a medial-to-medial lithofacies contact. Lithologically, the contact in the proximal lithofacies was sandier and thinner, but where the bounding surface was fairly thick (>0.30 ft) it showed an increase in finer-grained rocks. The amount of silt and shale within the bounding surface is related more to the thickness of the surface than the over- and underlying lithofacies designations.

Reservoir Modeling

During the quarter work, focused on two- and three-dimensional, fluid-flow modeling. Input parameters for both fluid and rock properties have been finalized for a plausible set of reservoir conditions. Simulations are being made to explore the way that outcrop-based data might be used to improve predictive simulations that, in turn, are needed to plan reservoir development. The

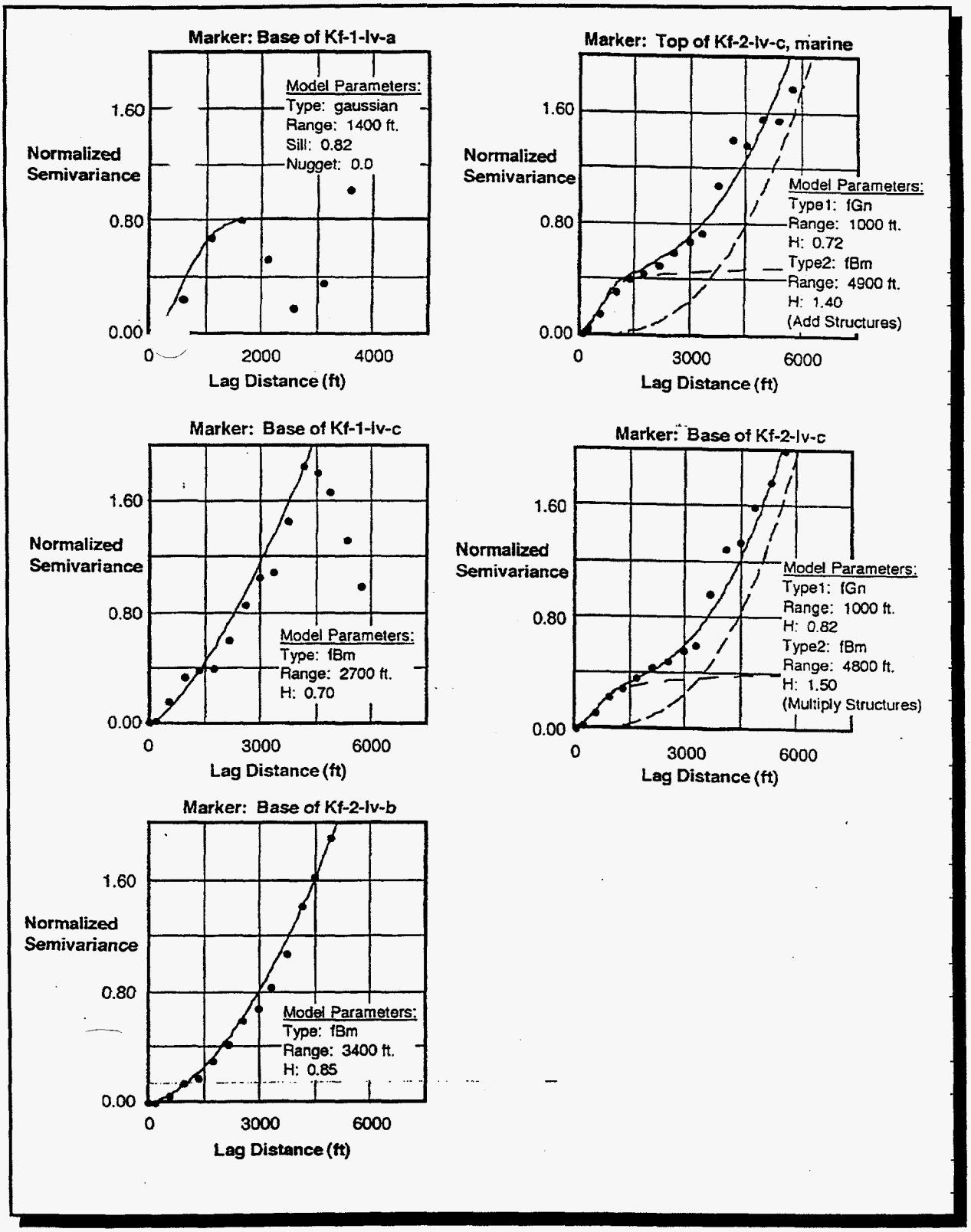

Fig. 4. Variograms of selected parasequence surfaces mapped in the Kf-1-Iv and Kf-2-Iv parasequence sets, Ivie Creek case-study area. In variograms on right, the overall model is represented by a solid line generated by adding or multiplying the type 1 (fGn or fractile Gaussian model) and type 2 (fBm fractile Brownian model) models represented by the dashed lines.

location and size of the two- and three-dimensional simulation domains are shown in Figs. 1 and 5. All flow simulations are run using the TETRAD black oil simulator.

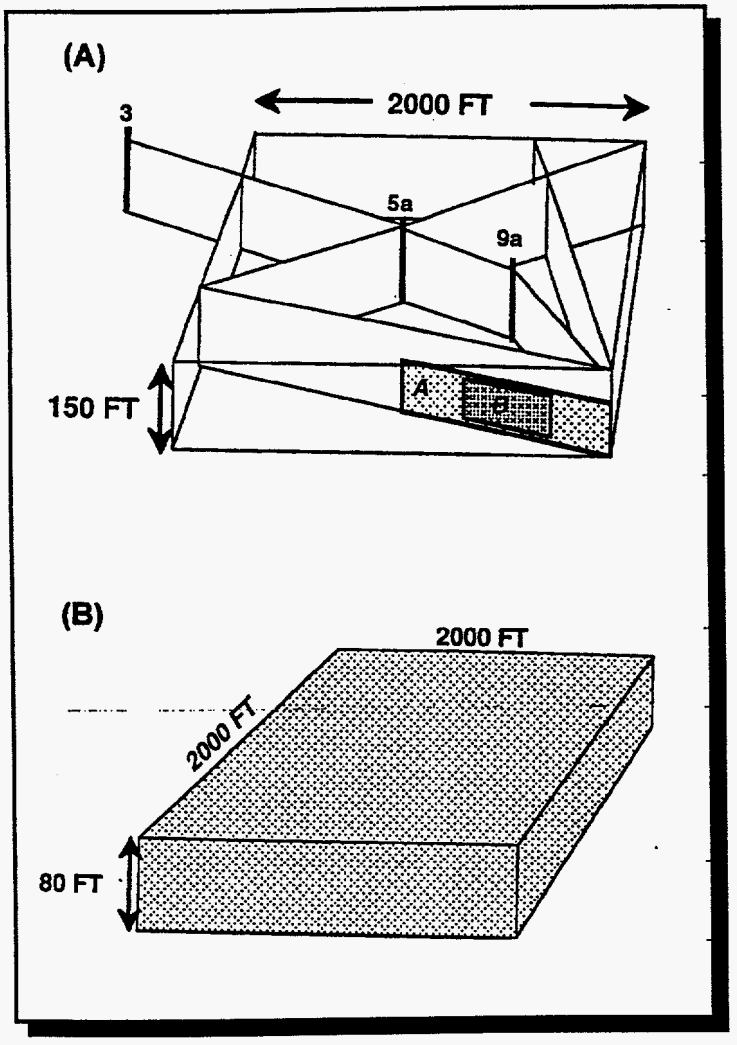

Fig. 5. (A) Sketch showing geological cross sections constructed within the Kf-1-Iv parasequence set within the three-dimensional model region. Two-dimensional, vertical modeling domains "A" and "B" are indicated along a geological cross section constructed from detailed photomosaic mapping Drill holes Nos. 3, 5a, and 9a are tied into the cross section. (B) Sketch of three-dimensional modeling volume used in simulating fluid flow through the Kf-1-Iv parasequence set exposed at the Ivie Creek case-study area.

The vertical, two-dimensional model domains (Fig. 5A) capture important elements of the transition from proximal to distal fluvial-deltaic lithofacies exposed along Highway I-70 in the Ivie Creek case-study area. In particular, these model domains enable one to explore how clinoform geometry and the inferred properties of the intervening bounding layers might influence the flow of oil and water at the interwell scale. Detailed geological mapping and the results of outcrop-based permeability testing provide a foundation for assigning petrophysical properties within the model domains.

The three-dimensional model domain measures 2000 ft by 2000 ft by 80 ft (Fig. 5B). Within this volume, the detailed distribution of lithofacies types of the Kf-1-Iv parasequence set has been inferred from a three-dimensional grid of 20 ft by 20 ft by 4-ft cells using the cross sections shown in Figs. 1 and 5A.

Assumed Reservoir Conditions

All simulations (both two- and three-dimensional modeling) are performed by imposing the hydraulic stresses associated with secondary recovery on a simulation volume in which uniform initial fluid pressures and saturations are defined. This approach avoids the excessive computational burden associated with determining steady-state reservoir pressures and fluid saturations that would have prevailed prior to implementing primary recovery. Similarly, the computational cost associated with calculating oil saturations at the end of primary production is avoided by assuming a uniform oil saturation

prior to simulating a waterflood. In addition to reducing the computational burden, these assumptions provide a simplified and uniform basis for comparing the results of waterflood simulations performed for a series of different petrophysical models. If the processes of reservoir filling and primary recovery were simulated for each petrophysical model, a different distribution of oil saturation would be computed as the initial conditions assigned when a simulated waterflood is initiated. The resulting variation in the initial conditions would complicate efforts to establish how each petrophysical structure influences the waterflooding process.

Finally, by restricting these simulations only to the waterflood phase the need to simulate gas production is avoided because fluid pressure reductions are minimal during waterflood which is not the case in the primary production phase. In these simulations the TETRAD simulator is operated in a mode that prohibits gas from coming out of solution. In order to justify this assumption, the minimum production-well, bottom-hole pressure is fixed at 2685 pounds per square inch absolute (psia) in the model. Because this pressure is the bubble point of black oil, it becomes impossible for pressure to drop below the bubble point anywhere in the reservoir at any time during a simulation.[1]

The reservoir is assumed to be initially saturated with both oil and water but no gas. Oil and water densities are assigned values of 45.0 and 62.14 lb/ft^3, respectively. A nominal reservoir pressure of 5000 pounds per square (psi) is assumed. This pressure corresponds to an approximate reservoir depth of 13,000 ft. A reservoir temperature of 60þC is assumed.

Fluid and Rock Properties

Relative Fluid-Permeability Curves. Predicted reservoir performance can depend strongly on the shapes of oil and water relative-permeability curves, particularly when spatial and temporal variations in saturation are pronounced. Thus, defining relative permeability relationships typical of fluvial-deltaic reservoir rocks is crucial for obtaining reliable performance predictions at various scales of permeability averaging. The water-wet Berea Sandstone is used as the prototype relative-permeability model for assessing production performance in the Ferron Sandstone because its hydraulic properties are widely documented in the literature and it is believed to represent a classic example of a consolidated sandstone.

Prototype relative-permeability data for the Berea Sandstone are available from a series of laboratory tests using brine and air as the wetting and non-wetting fluid phases, respectively.[2] Because these data were obtained for brine and air, they are not strictly applicable to the water-oil system of interest during the reservoir simulations. Thus, the Berea data was used to transform brine-air relative-permeability data obtained for samples of Ferron Sandstone into usable quantities through a two-step approach. The first step involves relating Berea brine-air relative permeabilities to Ferron brine-air relative permeabilities through the parameter þ used to fit the Brooks-Corey relations:

$$k_{rw} = S_e^{(2+3þ)/þ} \qquad (1)$$

$$k_{ro} = (1. - S_e)^2 * (1. - S_e)^{(2+þ)/þ} \qquad (2)$$

where: $S_e = (S_w - S_{wc})/(1. - S_{wc})$ is effective saturation, S_w and S_{wc} are actual and residual (connate) water saturations, and K_{rw} and K_{ro} are relative water and oil permeabilities.

After a value of þ was fit to the Berea brine-air relative permeability data and another value fit to the Ferron brine-air relative permeability data, the ratio of the two parameters was estimated in order to determine the fractional change in þ required to adjust the Berea curves for Ferron conditions. These fractional changes were obtained for 'average' Ferron brine-air data, as well as for proximal, medial, and distal subsets of the Ferron brine-air data, as determined from reported absolute brine permeabilities.[2] Since þ is a measure of the degree of linear behavior in the Brooks-Corey relations and the Berea Sandstone is relatively well-sorted compared to the Ferron Sandstone, all þ-adjustment ratios were less than 1.0. The resulting ratios were then used to adjust þ estimated from fitting another Brooks-Corey curve to the Berea oil-water relative permeability data obtained from three-phase relative permeability plots with a gas saturation of 0%.[3] Finally, the adjusted values of þ were used to generate Ferron Sandstone relative permeability curves for the average, proximal, medial, and distal clinoform lithofacies cases.

Capillary Pressure. Estimated values of capillary pressure in Ferron rocks, or the difference in pressure across the oil-water interface, were obtained from the standard water-wet Fatt and Dykstra relation provided in tabular form by Honarpour.[3] In a water-wet reservoir, a decrease in water saturation causes a decrease in curvature radius for water and a corresponding increase in capillary pressure. Table 1 shows the values of capillary pressure as a function of water saturation used in the Ferron Sandstone simulation studies.

TABLE 1

Capillary Pressure (P_c) as a Function of Water Saturation (S_w)

S_w	0.0	0.1	0.2	0.3	0.4	0.5	0.6	0.7	0.8	0.9	1.0
P_c (psi)	2.52	2.52	2.52	1.68	1.45	1.30	1.16	1.06	0.97	0.87	0.77

Pressure-Volume Data. Pressure-volume (PV) data relate oil production volumes at the ground surface to oil reservoir volumes at various reservoir pressures. The PV data used in this study (Table 2) are the same as those used in conducting a series of black oil simulations for the *Comparative Solution Project*.[4] Table 2 summarizes formation volume factors, solution-gas ratios, and fluid viscosities as a function of total reservoir pressure. Note that, because reservoir pressure is never allowed to drop below the bubble point during any point in the simulations, much of the table was never accessed during the TETRAD runs.

TABLE 2

Pressure-Volume Data

Pressure (psia)	BW (stb/rb)	EG	BO (stb/rb)	RS	CR	μ_w (cP)	μ_g (cP)	μ_o (cP)
14.7	1.0410	1.069	1.062	1.0	0	0.31	1.0	1.040
264.7	1.0403	14.728	1.150	90.5	0	0.31	1.0	0.975
514.7	1.0395	28.388	1.207	180.0	0	0.31	1.0	0.910
1014.7	1.0380	55.711	1.295	371.0	0	0.31	1.0	0.830
2014.7	1.0350	110.352	1.435	636.0	0	0.31	1.0	0.695
2514.7	1.0335	137.641	1.500	775.0	0	0.31	1.0	0.641
3014.7	1.0320	164.914	1.565	930.0	0	0.31	1.0	0.594
4014.7	1.0290	219.615	1.695	1270.0	0	0.31	1.0	0.510
5014.7	1.0258	274.434	1.827	1618.0	0	0.31	1.0	0.449
9014.7	1.0130	461.419	2.357	2984.0	0	0.31	1.0	0.203

BW = water formation factor (stb/rb)
EG = gas expansion factor
BO = oil formation factor (stb/rb)
RS = gas-solution ratio
CR = condensate ratio
μ_w = water viscosity (cP)
μ_g = gas viscosity (cP)
μ_o = oil viscosity (cP)

Two-Dimensional Simulations

To date, all two-dimensional simulations have been performed within a relatively small (330 ft horizontal by 48 ft vertical), prototypical model domain (Fig. 6) to gain confidence in the performance and use of TETRAD. Once the preliminary simulations are complete, the larger simulation domains will be initiated.

The results of the TETRAD simulation are shown in Fig. 7. Water is injected from a well located on the left boundary. A short (single grid block) perforated interval is centered in the reservoir. Oil is produced from a short (single grid block), centered interval perforated in a well located on the right boundary. Fig. 7 shows the distribution of oil saturation computed at several time steps using TETRAD.

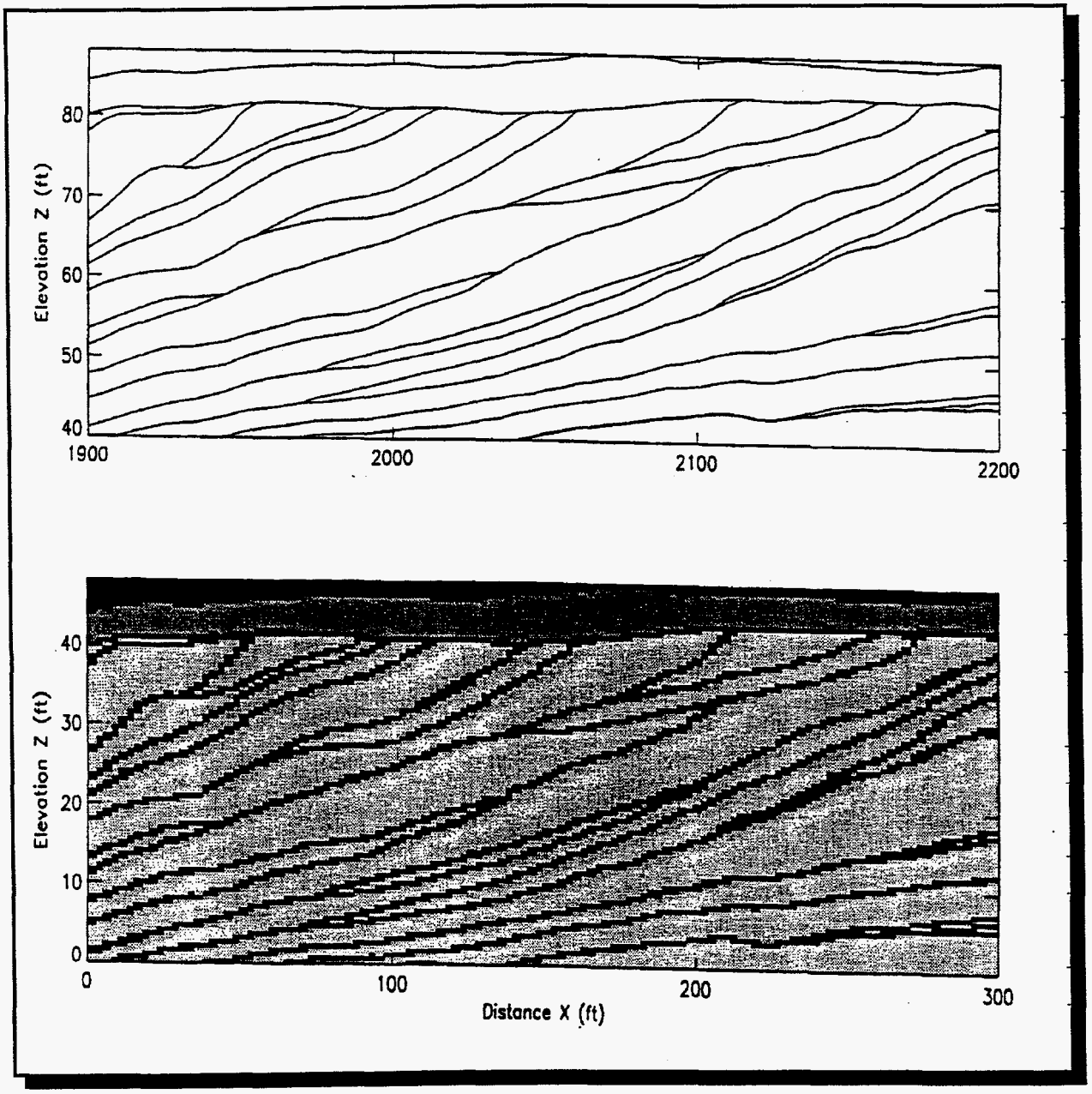

Fig. 6. Prototypical two-dimensional modeling domain showing the scaled line drawing to capture the geometry of the clinoform lithofacies and the corresponding, digitally gridded representation of the original line drawing.

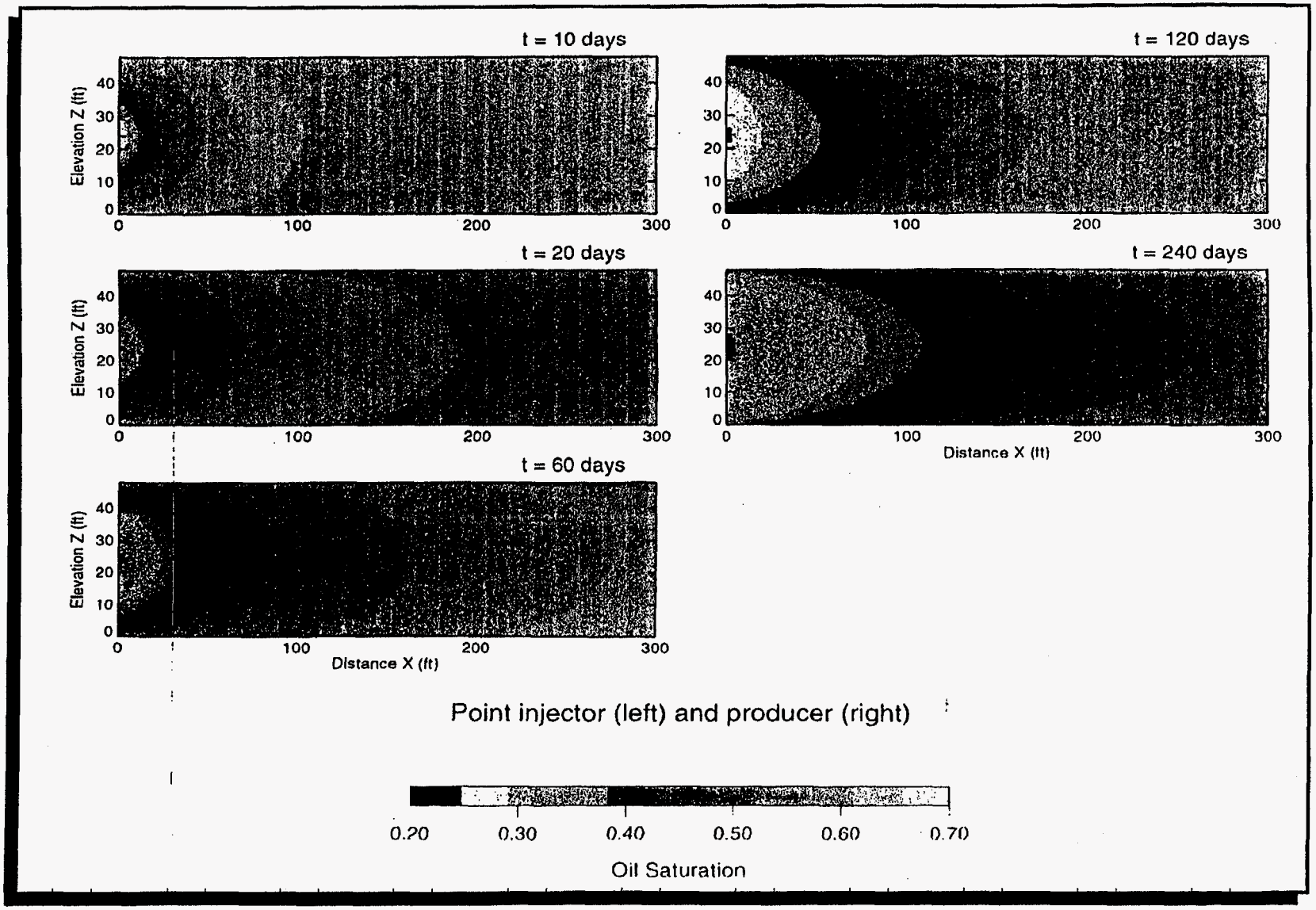

Fig. 7. Distributions of oil saturation as a function of time, computed using TETRAD, within a domain wit h homogeneous permeability (20 md) and porosity (0.50). Water is injected over a short interval centrally located alon the left boundary and oil is produced over a similarly located interval on the right boundary.

The prototypical model domain shown in Fig. 6 represents a portion of the Ivie Creek case-study area evaluated in detail. The algorithms needed to translate the scaled line drawings of clinoform boundaries (represented in the upper half of Fig. 6) into a corresponding, gridded distribution of petrophysical parameters (shown in the lower half of Fig. 6) were developed using this test domain. The algorithms provide an automated procedure for the following:

- converting the line drawings to individual polygonal elements (for example individual clinoform shapes),
- gridding the interiors of individual clinoforms,
- distinguishing between grid blocks representing clinoform boundaries and clinoform interiors,
- individually populating each clinoform with porosity values, relative permeability curves, and capillary pressure curves, and
- merging the gridded petrophysical distributions created for each clinoform into a single, heterogeneous model domain.

The lower half of Fig. 6 shows the results of this procedure. In this case, the parameter population is very simple; the gray clinoforms have a constant permeability of 20 md and the intervening, black boundary layers are assigned a constant permeability of 0.1 md. A porosity of 0.50 is assigned throughout the domain. Note that the black region at the top of the model domain is a null region that does not actively participate in the simulation. Improved algorithms that allow variable properties to be assigned within each clinoform are under development.

The progress of a waterflood through the model domain shown in Fig. 6 is simulated by injecting water along the left boundary of the domain and producing oil along the right boundary. Both the injector and producer are perforated across the entire thickness of the reservoir. A uniform, initial oil saturation of 0.70 is assumed with an inferred reservoir pressure of 5000 psia. The results of the TETRAD simulation are shown in Fig. 8. The impact of the clinoform architecture on the progress of the waterflood is evident. For example, the permeability contrast between the clinoform interiors (20 md) and the boundary layers (0.1 md) focuses flow within individual, dipping clinoforms. Once flow is established within a clinoform the water moves up dip to the producing well. The presence of the dipping, lower permeability bounding layers cause cumulative oil production computed from this simulation to be 20% less than that computed for the corresponding homogenous domain subjected to the same injection/production conditions.

Three-Dimensional Simulations

The primary goal of the three-dimensional reservoir simulation studies is to assess the dependence of predicted reservoir performance on the scale at which the three-dimensional spatial distribution of permeability is averaged. Three, three-dimensional styles of permeability structure are being simulated: homogeneous, layered heterogeneous, and detailed styles. If the measures of reservoir performance computed for each style are similar, one would conclude that there is little added value to collecting the outcrop information that was used to construct the detailed petrophysical model. If, on the other hand, the computed measures of reservoir performance differ dramatically from style to style, outcrop-based reservoir analog studies may be valuable.

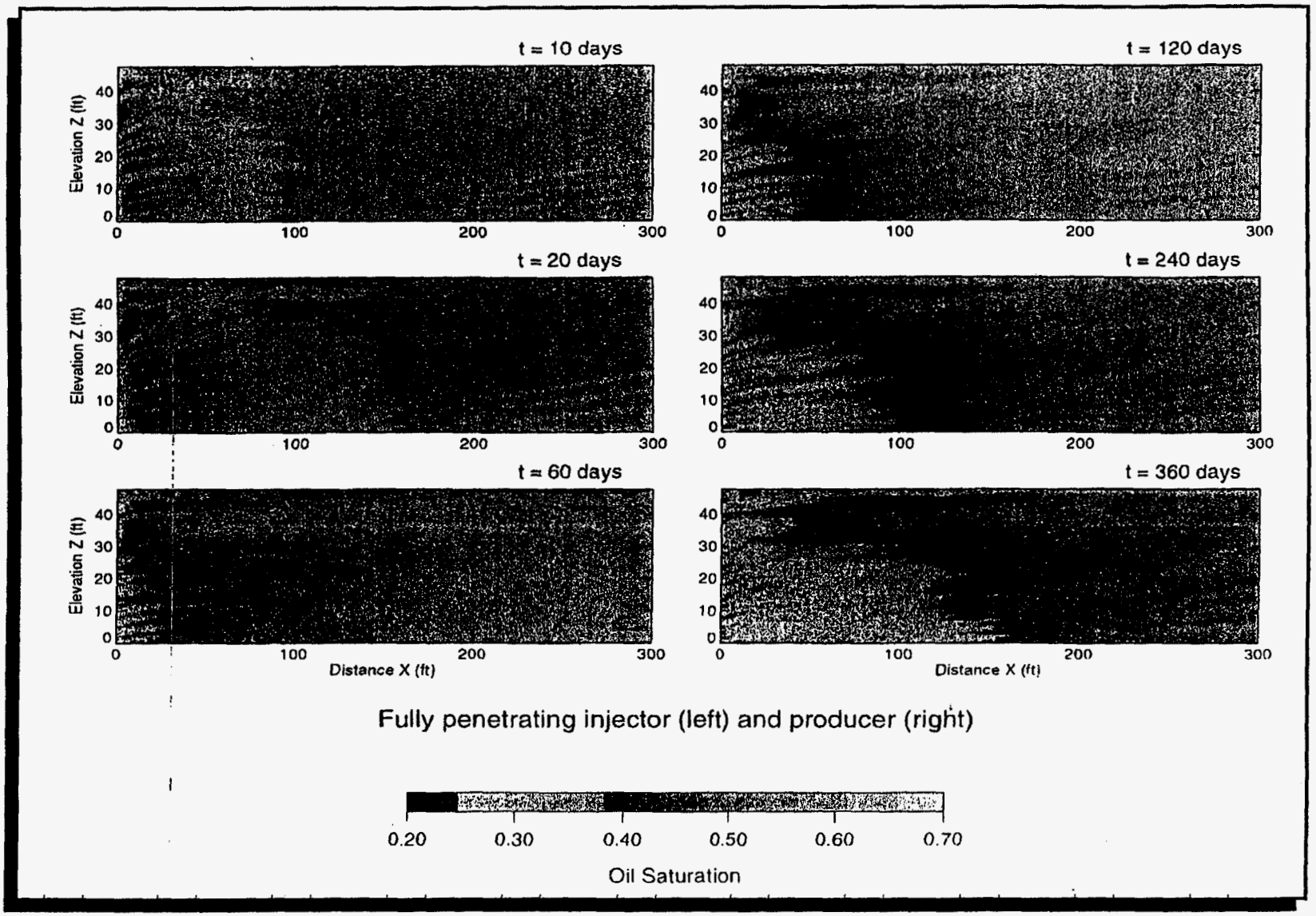

Fig. 8. Dist ributions of oil saturation as a function of time, computed using TETRAD, within the prototypical heterogeneous model domain shown in Fig. 6. Water is injected over the entire reservoir thickness on the left boundary and oil is produced over a similar interval on the right boundary.

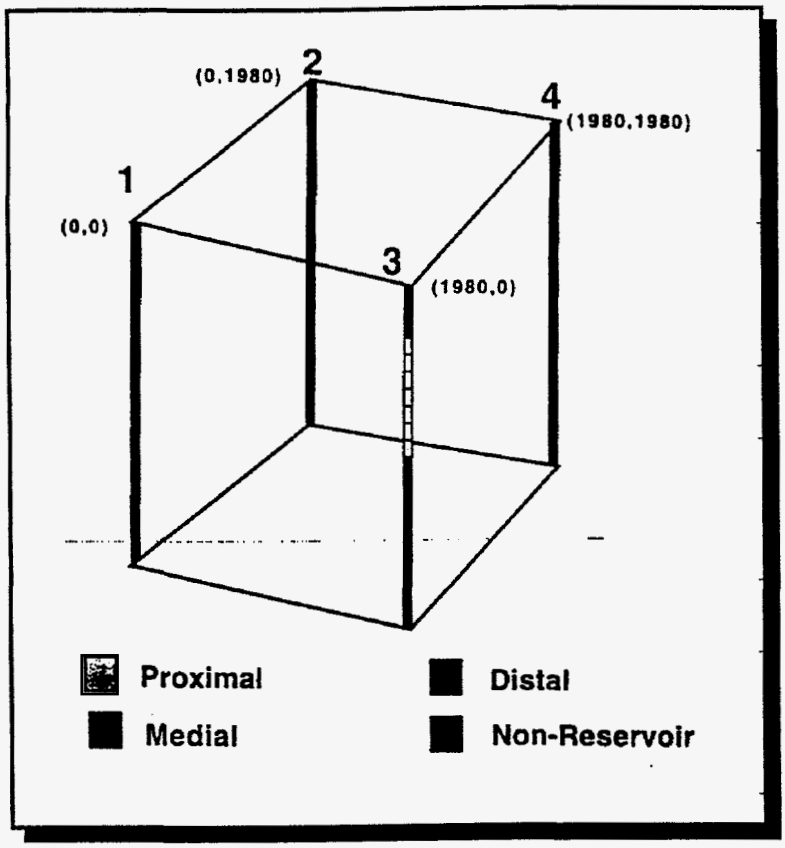

Fig. 9. Clinoform lithofacies distributions obtained by "drilling" and sampling four vertical "wells" in the detailed three-dimensional lithofacies model.

Each style of permeability structure is derived from the detailed three-dimensional lithofacies distribution constructed during the course of the Ferron outcrop analog study. Both the homogeneous and layered permeability structures represent the results of relatively simple permeability averaging techniques commonly used by petroleum engineers.

The layered permeability structure is obtained by interpolating lithofacies sampled from four hypothetical wells "drilled" vertically at the corners of the gridded three-dimensional representation of the detailed lithofacies distribution (Fig. 9). These wells might be viewed as the four producers that would be installed in a reservoir prior to adding a central injection well to complete a five-spot production pattern. Unlike the more detailed or fully homogeneous distributions, this intermediate distribution contains an inherent layering imposed in the process of interpolating lithofacies between wells. Fig. 10 shows the simple lithofacies structure inferred along two diagonal cross sections cutting through the three-dimensional simulation volume shown in Fig. 5.

In the homogeneous permeability structure case, a single representative value of permeability is assigned to the entire simulation volume to yield an end-member case with maximum averaging of permeabilities associated with the detailed lithofacies distribution. This computed effective permeability for the model volume was not obtained by applying formal homogenization techniques. Instead, it was estimated as the geometric mean of the detailed permeability structure contained within the entire three-dimensional, detailed lithofacies model.

A single five-spot waterflood production strategy is used to impose the secondary recovery process within the homogeneous three-dimensional model domain. This five-spot pattern encompasses the entire three-dimensional, 2000-ft by 2000-ft volume in the horizontal plane with a vertical thickness of 80 ft (Fig. 11). The horizontal symmetry of the production pattern, coupled with the intrinsic symmetry associated with the homogeneous reservoir properties, makes it possible to invoke ¼-volume, horizontal symmetry considerations. An initial uniform reservoir pressure of 5000 psia and initial uniform water and oil saturations of 0.5 were assigned throughout the ¼-volume reservoir prior to each simulation. In each simulation, water

is injected through the central well (corner well in the ¼-volume domain) at a rate of 0.0001 pore volumes/day (PV/day),

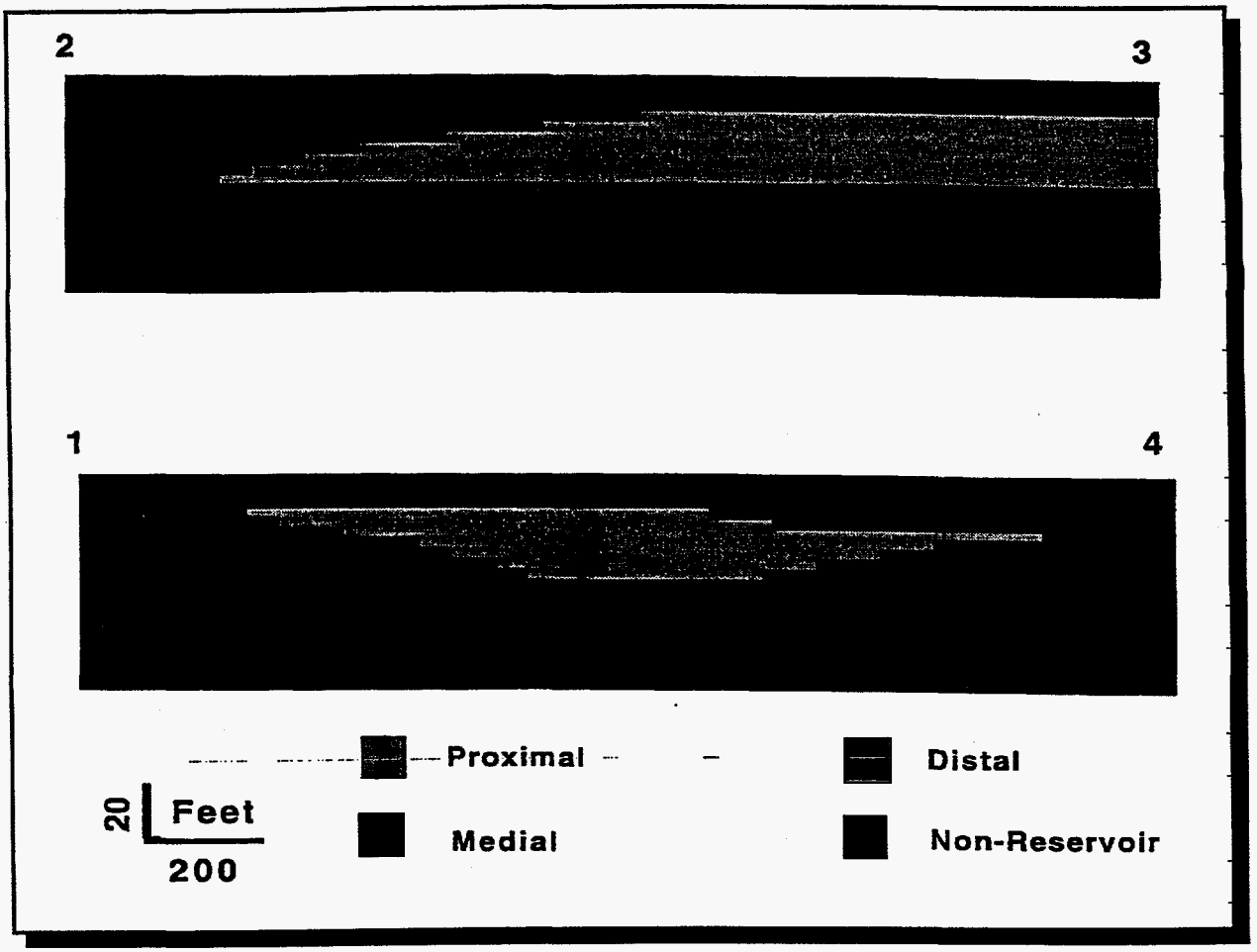

Fig. 10. Inferred structure of lithofacies along cross sections cut diagonally through the four-well pattern shown in Fig. 9.

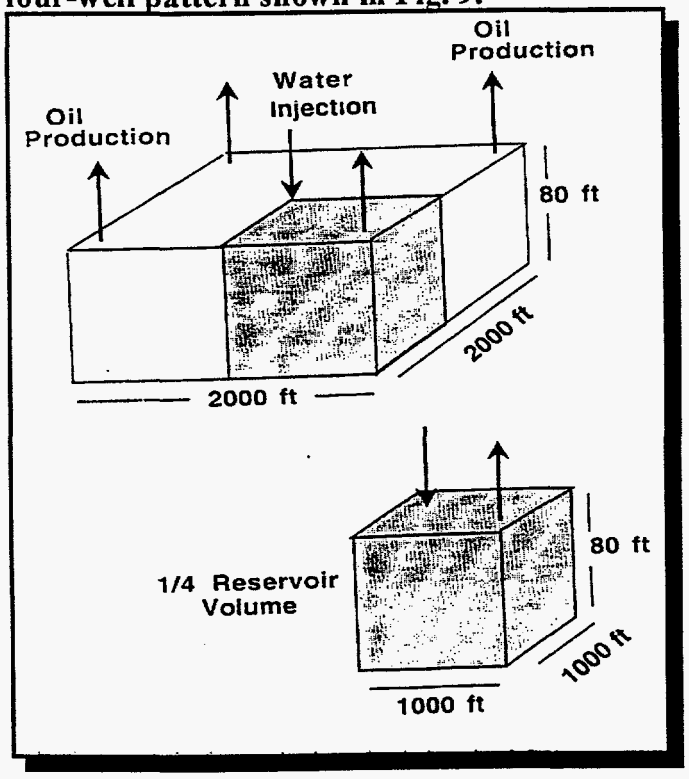

Fig. 11. Production scenario used when simulating the three-dimensional homogeneous case.

constrained by a maximum bottom-hole injection pressure constraint of 6000 psia. Production at the single corner well in the ¼-volume is driven by water injected at the opposite corner well. Review of permeability-porosity data collected in the course of the project suggests the following relationship:

$$\log k_{abs} = (22.72 * \text{þ}) - 2.64 \quad (3)$$

where þ = porosity expressed as a fraction and k_{abs} = absolute permeability (md). This relationship is used to compute porosity values where corresponding to values of k_{abs} are estimated.

Given that a large number of model runs are anticipated during future

sensitivity analyses, it is necessary to determine the minimum number of nodes required to discretize the pressure equations accurately over space. This is especially true for three-dimensional simulations, which can be extremely computationally intensive. In general, the degree of spatial resolution required will depend on spatial properties of both the physical system being modeled and the flow geometry imposed on the physical system. Steep pressure gradients and extreme variations in permeability, for example, will usually require fine grid resolution. Low gradients and small, gradual changes in permeability over space can be accurately preserved using coarser resolution.

To generate the steepest horizontal gradients common to all three permeability distributions, the geometric mean associated with the lowest permeability, clinoform distal lithofacies (1.48 md) was assigned to the homogeneous model domain. A fairly large water injection rate of 0.0001 PV/day was imposed at the central water-injection well. This combination of low k_{abs} and high injection rate provides worst-case conditions from the perspective of defining a minimum acceptable grid resolution. Specifying initially uniform water and oil saturations, which tend to establish a piston-like pattern of fluid displacement, also contribute to this worst-case scenario.

A number of homogeneous permeability simulations were made using several uniform grid-spacing geometries. In the later stages of each simulation, however, mass balance errors were found to increase beyond acceptable limits. As a consequence, the horizontal grid spacing (Fig. 12) is varied to alleviate the numerical problems associated with preserving steep horizontal gradients while leaving the computational burden unchanged. A 2-ft grid spacing is assigned near the injection and production wells. The horizontal grid spacing gradually increases to 202 ft at the midpoint between the injection and production wells. This discretization scheme produces a grid with 20 ft by 20 ft by 10 ft grid blocks (4000 finite difference nodes) within the ¼-volume. Small mass balance errors are computed throughout the model domain using this variable grid. This result suggests that the 4000-node, variable-spacing discretization may be capable of accurately preserving the steepest horizontal pressure gradients that are likely to evolve while simulating each of the three different styles of permeability structure. Note that, when simulating the two heterogeneous styles, one can no longer invoke the ¼-symmetry. As a consequence, when modeling these styles it will be necessary to use at least 16,000 nodes.

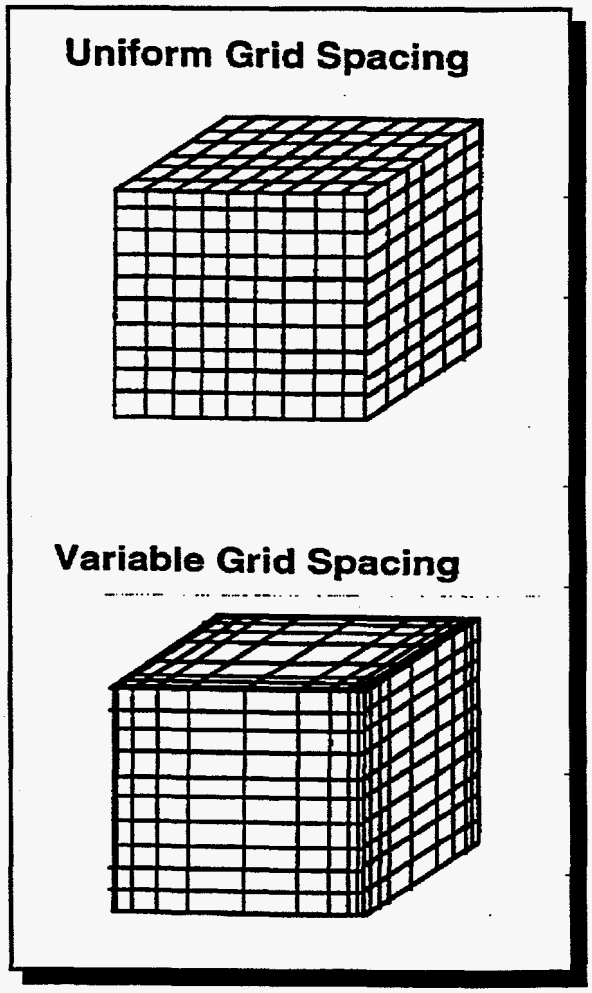

Fig. 12. Grid spacings used in the ¼-volume three-dimensional model domain shown in Fig. 11.

Using the optimal grid design based on worst-case conditions (minimum-permeability, maximum pressure-gradient, piston-like displacement), a set of sample results are computed for the homogeneous, ¼-volume, model domain. In this case a homogeneous geometric mean permeability of 3.13 md is assigned to represent the mean permeability of the full three-dimensional volume. A corresponding porosity of 0.138 is estimated using the linear correlation relation given by equation 3. Computed three-dimensional distributions of oil saturation are shown in Fig. 13 for a series of points in time ranging from 6 months to 20 years. In each three-dimensional saturation plot, the water-injection well is located at the left corner of the model domain, and the oil production well is located in the right corner. White areas correspond to high oil saturations. Thus, one can see the progress of the waterflood through the domain as the dark

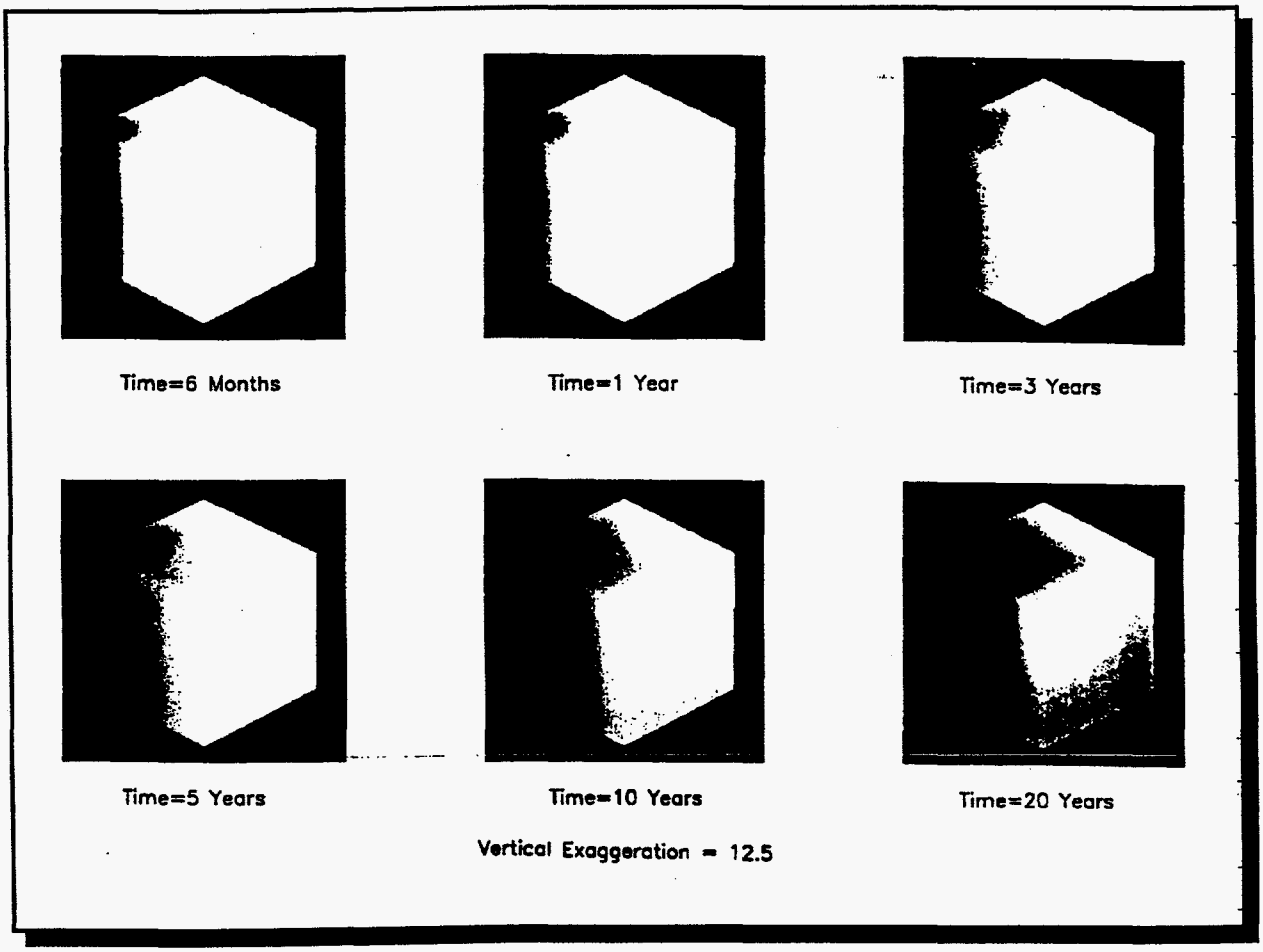

Fig. 13. Distribution of oil saturation as a function of time for variable grid (horizonta plane) within the three-dimensional model domain. The expanding dark region represents the progress of the water phase through the reservoir during the waterflood. Injectio occurs on the left corner of the ¼-volume block. Production occurs on the right corner.

area, corresponding to high water saturation, expands to fill the model domain.

The results of the preliminary three-dimensional simulation performed for the homogeneous model domain are summarized in the plots of water-injection rate, oil-production rate, and water cut (Fig. 14). Note that, because we have simulated only one fourth of the full three-dimensional volume, each rate must be multiplied by 4 to obtain reservoir performance measures for the full 2000-ft by 2000-ft by 80-ft simulation volume.

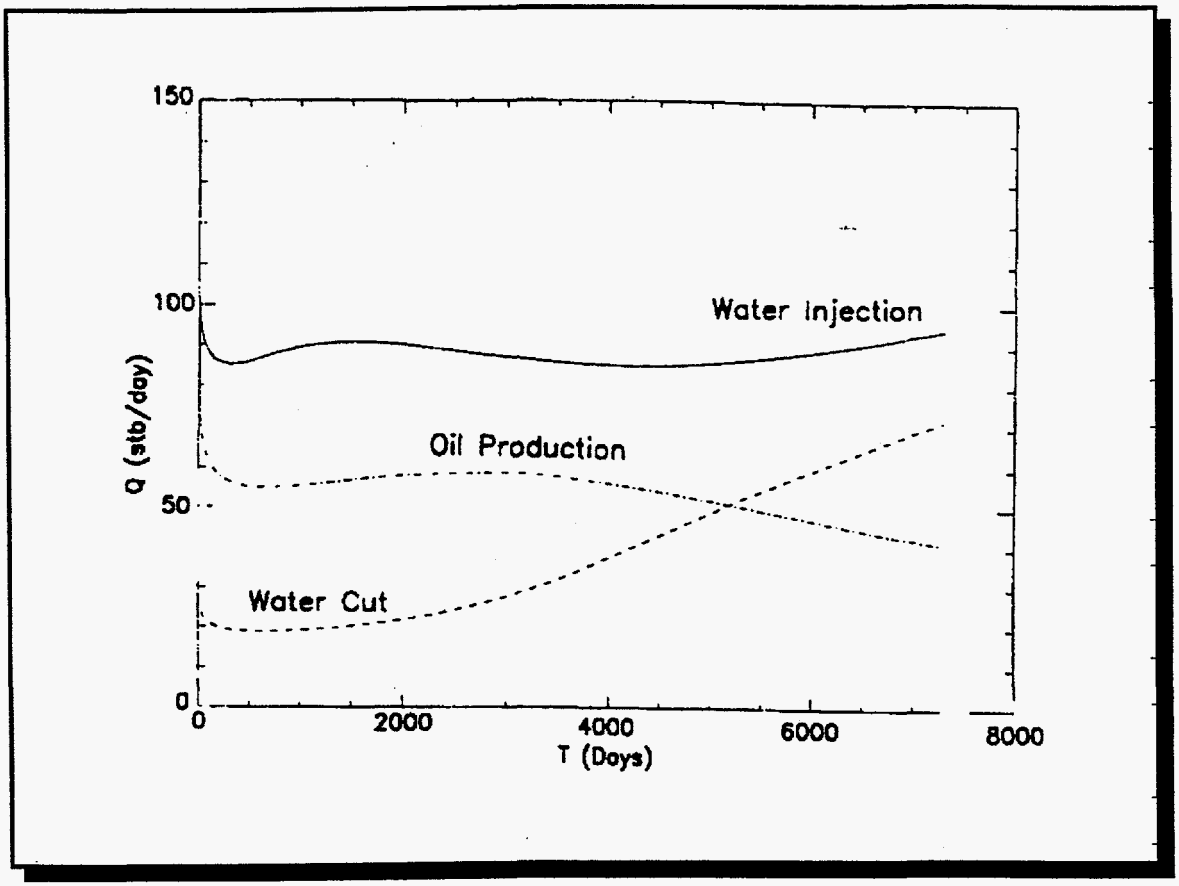

Fig. 14. Summary plots of water-injection rate,water cut, and oil-production rate as a function of time; computed for the three-dimensional simulation shown in Fig. 13.

Technology Transfer

The UGS and its partners continued to prepare presentations of the final results of the project to both academia and industry. Field trips covering the regional stratigraphy and case-study areas will be conducted during the 1997 Geological Society of America (GSA) and 1998 American Association of Petroleum Geologists (AAPG) annual national meetings. The field trip road logs and Ferron interpretations will be published in a two-volume GSA guidebook. A short course presenting reservoir modeling and simulation results will also be offered during the AAPG meeting. The meetings will be held in Salt Lake City, Utah, October 19-22, 1997 (GSA) and

May 20-23, 1998 (AAPG). The field trip and short course presented at the AAPG meeting will sponsored by both the UGS and the National Petroleum Technology Office - DOE.

The UGS has made the collection of core from drill holes in the project area publicly available at the UGS Sample Library. The Sample Library provides service to all interested individuals and companies who require direct observation of actual samples for their research or investigations. High-quality photographs of the slabbed core surfaces are available for a nominal fee. The project core may be examined on site or borrowed for a period of six months. Destructive sampling is occasionally permitted with approval. The UGS requires copies of all reports, photographs, and analyses from these investigations; this information can be held confidential for one year upon request.

References

1. W. D. McCain, Jr., *The Properties of Petroleum Fluids*, Pennwell Publishing Co., Tulsa, 1990.

2. M. A. Miller, J. Holder, H. Yang, Y. Jamal, and K. E. Gray, Petrophysical and Petrographic Properties of the Ferron Sandstone, Gas Research Institute *Topical Report* Gri-93/0219: (September 1993).

3. M. Honarpour, L. Koederitz, and A. H. Harvey, *Relative Permeability of Petroleum Reservoirs*, CRC Press, Boca Raton, 1986.

4. A. S. Odeh, Comparison of Solutions to a Three-Dimensional Black-Oil Reservoir Simulation Problem, *Soc. Pet. Eng.*, Paper 9723: (January 1981).